AD_____

Award Number: DAMD17-97-1-7195

TITLE: Determination of the Crystal Structure of Human Zn-Alpha
2-Gylcoprotein, A Protein Implicated in Breast Cancer

PRINCIPAL INVESTIGATOR: Pamela Bjorkman, Ph.D.
Dr. Arthur Chirino

CONTRACTING ORGANIZATION: California Institute of Technology
Pasadena, California   91125

REPORT DATE: August 2000

TYPE OF REPORT: Final

PREPARED FOR: U.S. Army Medical Research and Materiel Command
Fort Detrick, Maryland   21702-5012

DISTRIBUTION STATEMENT: Approved for Public Release;
Distribution Unlimited

The views, opinions and/or findings contained in this report are
those of the author(s) and should not be construed as an official
Department of the Army position, policy or decision unless so
designated by other documentation.

1

20010220 028

REPORT DOCUMENTATION PAGE

Form Approved
OMB No. 074-0188

Public reporting burden for this collection of information is estimated to average 1 hour per response, including the time for reviewing instructions, searching existing data sources, gathering and maintaining the data needed, and completing and reviewing this collection of information. Send comments regarding this burden estimate or any other aspect of this collection of information, including suggestions for reducing this burden to Washington Headquarters Services, Directorate for Information Operations and Reports, 1215 Jefferson Davis Highway, Suite 1204, Arlington, VA 22202-4302, and to the Office of Management and Budget, Paperwork Reduction Project (0704-0188), Washington, DC 20503

1. AGENCY USE ONLY (Leave blank)	2. REPORT DATE August 2000	3. REPORT TYPE AND DATES COVERED Final (1 Aug 97 - 31 Jul 00)

4. TITLE AND SUBTITLE
Determination of the Crystal Structure of Human Zn-Alpha 2-Gylcoprotein, A Protein Implicated in Breast Cancer

5. FUNDING NUMBERS
DAMD17-97-1-7195

6. AUTHOR(S)
Pamela Bjorkman, Ph.D.
Dr. Arthur Chirino

7. PERFORMING ORGANIZATION NAME(S) AND ADDRESS(ES)

California Institute of Technology

Pasadena, California 91125

E-MAIL:
bjorkman@cco.caltach.edu

8. PERFORMING ORGANIZATION REPORT NUMBER

9. SPONSORING / MONITORING AGENCY NAME(S) AND ADDRESS(ES)

U.S. Army Medical Research and Materiel Command
Fort Detrick, Maryland 21702-5012

10. SPONSORING / MONITORING AGENCY REPORT NUMBER

11. SUPPLEMENTARY NOTES
This report contains colored photos

12a. DISTRIBUTION / AVAILABILITY STATEMENT
Approved for public release; distribution unlimited

12b. DISTRIBUTION CODE

13. ABSTRACT *(Maximum 200 Words)*

Zn-α_2-glycoprotein (ZAG) is a 41 kDa soluble protein whose sequence and domain organization are surprisingly similar to those of the membrane glycoproteins of the major histocompatibility complex (MHC). MHC molecules function in the presentation of peptide antigens to cytotoxic T cells during immune surveillance, but recent data indicate that ZAG stimulates lipid degradation in adipocytes and causes the extensive fat losses associated with some advanced cancers. In addition, ZAG is found in high concentrations in 40% of mammary carcinomas, as well as in cysts from breast gross cystic disease. These data suggest that ZAG participates in the development of breast diseases including breast carcinomas. We purified ZAG from human serum and solved the crystal structure to 2.8 Å resolution. ZAG resembles a class I major histocompatibility complex heavy chain, but ZAG does not bind the class I light chain β_2-microglobulin. The ZAG counterpart of the MHC peptide binding groove contains electron density corresponding to a hydrophobic, non-peptidic compound that may be implicated in lipid catabolism under normal or pathological conditions. We have initiated mass spectrometry assays to identify the ligand and are testing the ability of hydrophobic small molecules to bind to serum-derived ZAG and to ZAG produced in bacteria, which presumably does not contain a hydrophobic ligand.

14. SUBJECT TERMS Breast Cancer			15. NUMBER OF PAGES 17
			16. PRICE CODE

17. SECURITY CLASSIFICATION OF REPORT Unclassified	18. SECURITY CLASSIFICATION OF THIS PAGE Unclassified	19. SECURITY CLASSIFICATION OF ABSTRACT Unclassified	20. LIMITATION OF ABSTRACT Unlimited

NSN 7540-01-280-5500

Standard Form 298 (Rev. 2-89)
Prescribed by ANSI Std. Z39-18
298-102

Table of Contents

THE THREE_DIMENSIONAL CRYSTAL STRUCTURE OF ZN-α2-GLYCOPROTEIN, THE MOLECULE RESPONSIBLE FOR CACHEXIA-RELATED FAT LOSS

Arthur J. Chirino, Luis M. Sánchez, Astrid Heikema*, and Pamela J. Bjorkman*

Division of Biology and the Howard Hughes Medical Institute*
California Institute of Technology
Pasadena, California, 91125

E-mail: art01@caltech.edu

Zn-α_2-glycoprotein (ZAG) is a 41 kDa soluble protein that is present in most bodily fluids. ZAG shares 30-40% amino acid sequence identity with the extracellular portions of class I major histocompatibility complex (MHC) heavy chains. MHC class I molecules bind antigenic peptides within their peptide binding grooves and present these peptides to T-cell receptors in order for the immune system to distinguish foreign from self, but ZAG has no known function in the immune system. Recently, ZAG was shown to cause extreme lipid depletion in patients with certain cancers [1]. Since upwards of 20% of cancer-related deaths are a direct result of the wasting syndrome, developing therapies to reduce the systemic strain associated with cachexia is of vital importance. In addition, ZAG's role in lipid metabolism and weight loss implies that ZAG may be of therapeutic benefit in controlling clinical obesity.

We set out to determine the three dimensional crystal structure of ZAG using x-ray diffraction methods in order to develop the structural framework required to design specific inhibitors of cachexia. ZAG was purified from human serum using immunoaffinity, ion-exchange, and hydrophobic chromatographies and single diffraction quality crystals of ZAG were grown [2]. The crystal structure was determined using the multiple isomorphous replacement method [3]. The 2.8 Å crystal structure of ZAG demonstrates the structural similarity between ZAG and MHC I molecules. While the α-helices comprising the sides of the peptide binding groove of MHC I molecules are similarly positioned as the analogous helices in ZAG, the overall shape and chemical nature of the grooves are different. In addition, unlike MHC I molecules, ZAG was shown to bind a small as yet unidentified non-peptidic ligand within its groove. The importance of this ligand in ZAG's structure and function is unclear, but it appears to be a hydrophobic small molecule that may be related to ZAG's role in lipid metabolism. In an on-going effort in our laboratory, we are analyzing ZAG extracts using various forms of mass spectrometry to identify the ligand.

In a colloboration with Dr. Malcolm Kennedy (University of Glasgow), we have used calorimetry and fluorescence experiments to examine the ability of fatty acid-related compounds to bind to ZAG. We have shown that ZAG binds DAUDA, a fluorescent fatty acid probe, whereas control proteins (class I MHC molecules and class I MHC homologs FcRn and HFE) show no detectable binding. Furthermore only ZAG shows any change in its intrinsic tryptophan fluorescence upon addition of fatty acids (oleic, arachidonic). We are currently trying to determine whether the ZAG groove is the binding site for DAUDA and other fatty acids.

We are also attempting to produce a ZAG molecule devoid of its endogenous ligand in order to evaluate the ligand's role in lipid breakdown. Obtaining a snap shot of ZAG's empty groove by solving a crystal structure of "empty" ZAG could be beneficial in designing drug compounds to block ligand binding. We have bacterially expressed human ZAG (bZAG) and successfully refolded the protein from inclusion bodies. Since bacteria and mammals utilize vastly different lipid metabolism pathways, the expectation is that bZAG's groove will be empty. While bZAG is not glycosylated, it is considerably more

thermal stable than ZAG isolated from human serum. We have obtained small crystals of bZAG alone and are attempting to grow bZAG crystals in complex with a number of compounds, including DAUDA and other fatty acids, to aid in the identification of the ligand bound to ZAG in human serum.

1) P. T. Todorov, et al., *Cancer Res.* **58**, 2353 (1998)

2) Sánchez, L.M., López-Otín, C., and Bjorkman, P.J. (1997) Biochemical characterization and crystallization of human Zn-α2-glycoprotein, a soluble class I MHC homolog. *Proc. Natl. Acad. Sci. USA* **94**: 4626-4630.

3) Sánchez, L.M., Chirino, A.J. & Bjorkman, P.J. (1999) Crystal structure of human Zn-α2-glycoprotein: a fat-depleting factor related to MHC molecules. *Science* **283**: 1914-1919.

Biochemical characterization and crystalization of human Zn-α2-glycoprotein, a soluble class I major histocompatibility complex homolog

LUIS M. SÁNCHEZ*, CARLOS LÓPEZ-OTÍN†, AND PAMELA J. BJORKMAN‡§

*Division of Biology 156-29 and ‡Howard Hughes Medical Institute, California Institute of Technology, Pasadena, CA 91125; and †Departamento de Bioquímica y Biología Molecular, Facultad de Medicina, Universidad de Oviedo 33006, Oviedo, Spain

ABSTRACT   Zn-α2-glycoprotein (ZAG) is a 41-kDa soluble protein that is present in most bodily fluids. In addition, ZAG accumulates in fluids from breast cysts and in 40% of breast carcinomas, which suggests that ZAG plays a role in the development of breast diseases. However, the function of ZAG under physiological and cancerous conditions remains unknown. Because ZAG shares 30–40% sequence identity with the heavy chains of class I major histocompatibility complex (MHC) proteins, we compared the biochemical properties of ZAG with those of classical class I MHC molecules. We purified human ZAG from breast cyst fluid and serum and produced a panel of anti-ZAG monoclonal antibodies. Binding assays and acid elution experiments revealed that, in contrast to class I MHC proteins, ZAG does not bind peptides or the class I light chain, β_2-microglobulin (β_2m). Nevertheless, CD studies indicated that ZAG is thermally stable in the absence of bound peptide or associated β_2m, as opposed to class I MHC molecules, which require the presence of both β_2m and peptides for stability. These data indicate that the function of ZAG has diverged from the peptide presentation and T-cell interaction functions of class I molecules. To gain insight into the function of ZAG and to compare the three-dimensional structures of ZAG and class I MHC molecules, we produced ZAG crystals that diffract beyond 2.7 Å and have initiated an x-ray structure determination.

Zn-α2-glycoprotein (ZAG) is a soluble protein that was originally isolated from human plasma (1). Its name derives from its tendency to precipitate with zinc salts, its electrophoretic mobility in the region of the α_2 globulins, and its 18% carbohydrate content. The function of ZAG is unknown, but several studies have shown that this protein is present in other bodily fluids, including sweat, saliva, cerebrospinal fluid, seminal plasma, milk, ammiotic fluid, and urine (2). In addition, ZAG is found at high concentrations in the fluid from breast cysts and in 40% of breast carcinomas (3–6). These findings, together with the fact that ZAG is induced by glucocorticoids and androgens in breast cancer cell lines (7), suggest that this protein may participate in the development of mammary diseases, including breast cancer.

Amino acid sequence analysis revealed that ZAG is surprisingly similar to class I major histocompatibility complex (MHC) proteins (8). Class I MHC molecules are heterodimers, consisting of a membrane-bound heavy chain noncovalently associated with β_2-microglobulin (β_2m), a soluble protein that serves as the light chain. Class I molecules bind peptides derived from intracellular proteins and present them to cyto-

toxic T cells during immune surveillance (9). Crystal structures reveal that they fold into a shape ideally suited for peptide binding. Two long α-helices form the sides of a groove within the first two domains (α_1 and α_2) of the heavy chain, and a β-pleated sheet forms the bottom. The β_2m light chain and the other domain of the heavy chain (α_3) lie underneath the α_1 and α_2 domains, with β_2m interacting simultaneously with the side of the α_3 domain and the bottom of the α_1-α_2 domain platform (reviewed in refs. 10 and 11). ZAG is composed of three domains that share 30–40% amino acid sequence identity with the three extracellular domains of class I heavy chains. This level of sequence identity is compatible with structural similarity, as shown by Chothia and Lesk (12).

Analysis of ZAG cDNA and genomic clones provided further data about the relationship between ZAG and class I MHC molecules (13). Similarities in exon organization, intron-exon junctions, and nucleotide sequence indicate that the coding regions of the ZAG gene are homologous to the first four exons of MHC genes, which encode the signal peptide and the three extracellular domains of the heavy chain. However, the ZAG gene does not encode transmembrane or cytoplasmic regions and lacks the regulatory and interferon consensus sequences that are conserved in typical MHC genes (13). In addition, the ZAG gene differs from class I genes in its lack of polymorphism and in its location outside of the MHC (14). The recent identification of cDNAs coding for ZAG in mice and rats (15, 16) shows that the divergence between ZAG and MHC molecules began at least 80 million years ago, before the evolutionary radiation of the placental mammals (17).

This work addresses how this divergence has affected the biochemical and structural characteristics of ZAG. We purified human ZAG from fluid obtained from breast cysts and from serum, produced anti-ZAG mAbs, and compared its properties with those of class I MHC molecules. In addition, as a first step in a three-dimensional structure determination, we produced crystals of ZAG that are suitable for an x-ray diffraction analysis.

MATERIALS AND METHODS

Materials. Fluid from breast cysts obtained from patients with breast gross cystic disease was kindly provided by F. Vizoso from Hospital de Jove (Gijón, Spain). Human serum was the gift of J. Goin, from Biocell Laboratories. Samples were stored at −20°C. Before use, fats and debris were removed by centrifugation at 10,000 × g and filtration through 0.2 μm filters. Human β_2m and anti-β_2m polyclonal antiserum were from Sigma. Chromatographic matrices and equipment were from Pharmacia. Antibody isotyping was performed with

Abbreviations: β_2m, β_2-microglobulin; MHC, major histocompatibility complex; ZAG, Zn-α2-glycoprotein; T_m, transition midpoint; neonatal FcRn, Fc receptor.
§To whom reprint requests should be addressed. e-mail: bjorkmanp@starbase1.caltech.edu.

a kit from GIBCO/BRL. ^{125}I-protein A was from Amersham. Native PAGE was performed using a PhastSystem (Pharmacia).

Purification of ZAG from Breast Cyst Fluid. Seventy-five milliliters of cyst fluid was loaded on a phenyl Sepharose column equilibrated with 50 mM sodium phosphate (pH 7), 0.75 M $(NH_4)_2SO_4$. The column was washed with 0.25 M $(NH_4)_2SO_4$ in sodium phosphate, and ZAG was eluted with 50 mM sodium phosphate (pH 7). Fractions containing ZAG were applied on a nickel-chelating Sepharose column equilibrated with 50 mM sodium phosphate (pH 7.5), 0.5 M NaCl. ZAG was recovered in the flowthrough, while contaminant proteins were retained on the chelating column. ZAG was further purified by chromatography on a Superdex 200 HiLoad FPLC column equilibrated in 20 mM Hepes (pH 7), 150 mM NaCl. Purified ZAG was desalted and concentrated using a Centricon-10 (molecular weight cutoff of 10,000) ultrafiltration device (Amicon) and stored in 20 mM Hepes (pH 7), 0.02% NaN_3 at 4°C.

Antibodies. Rabbit anti-ZAG polyclonal antiserum was produced as described (4). Female BALB/c mice (aged 5 weeks) were primed and twice boosted at 2-week intervals by intraperitoneal injection of 100 μg of purified ZAG in adjuvant. Serum was screened a week after each injection by ELISA as described (18). Three days preceding the fusion, one mouse was boosted with 100 μg of purified ZAG. Splenocytes from the boosted mouse were fused with HL-1 murine myeloma cells, and media from the hybridoma cultures were tested for antibodies against ZAG by ELISA. After subcloning positive clones at clonal density, ascites tumors were produced in pristane-primed BALB/c mice. Eight anti-ZAG mAbs produced by this fusion were subsequently characterized (Table 1). All antibodies are murine IgG_1-κ. Conditions for elution of ZAG were determined by ELISA as described (19).

Purification of ZAG from Human Serum. Seventy-five milligrams of the purified mAb 3C5 were coupled to a CNBr-activated Sepharose column according to the manufacturer's instructions. Two-hundred-fifty-milliliter aliquots of serum were loaded on the 3C5 immunoaffinity column equilibrated with 20 mM of sodium phosphate (pH 7.5), 0.5 M NaCl. After washing with the same buffer, ZAG was eluted with 20 mM sodium acetate (pH 4.5), 0.5 M NaCl into tubes containing Hepes (pH 7). Fractions containing ZAG were desalted and loaded on a Q Sepharose column equilibrated with 20 mM of piperazine (pH 5). For biochemical experiments, ZAG was eluted using 0.1 M NaCl in the piperazine buffer and stored as before. For crystalization, ZAG was eluted using a gradient from 0 to 50 mM NaCl in the piperazine buffer. Under these conditions, ZAG eluted in two peaks. The peak that eluted in higher salt was loaded on a Source phenyl column equilibrated with 50 mM sodium phosphate (pH 6), 0.75 M $(NH_4)_2SO_4$ and eluted with a gradient from 0.75 M to 0 M $(NH_4)_2SO_4$ in the same buffer. ZAG was further separated into two peaks that eluted with 0.56 M and 0.41 M $(NH_4)_2SO_4$, respectively.

Table 1. mAbs against ZAG

Clone name	Western blot	Immuno-precipitation	pH required for elution of ZAG
1B5	+	+	4.0
1D4	++	++	4.0
1E2	++	++	3.0
1H4	+	++	3.0
3C5	++	+	4.5
3F4	+/−	++	3.5
4E3	−	+	3.5
6G2	++	++	3.5

β_2m Binding Assays. For chromatographic experiments, 4 μg of ZAG were mixed with 1 to 30 μg of β_2m in 25 μl of Tris-buffered saline. After 6 h, the sample was injected on a SMART system Superdex 75 Precision column equilibrated in the same buffer. Absorbance was measured at 280 nm, and fractions were analyzed by SDS/PAGE. For immunoprecipitation assays, 1-ml aliquots of serum were incubated with 25 μl of protein A Sepharose for 30 min. After pelleting, supernatants were incubated for 1 h with 10 μg of polyclonal antiserum against ZAG or β_2m, followed by a 30-min incubation with protein A Sepharose. The resins were pelleted and washed with Tris-buffered saline containing 0.1% BSA, 0.1% SDS, 1% Nonidet P-40, and 1% sodium deoxycholate. The immunoprecipitated proteins were separated by SDS/PAGE and blotted onto nitrocellulose filters, which were incubated with antiserum against either ZAG or β_2m and developed with ^{125}I-protein A following published protocols (4).

Acid Elutions of ZAG or a Class I MHC Heterodimer (H-2K^d). Purified ZAG from serum or H-2K^d (a soluble version of the K^d heavy chain complexed with human β_2m (20); proteins were analyzed for the presence of bound peptides using established methods (21, 22). Aliquots of 1 mg of protein were diluted into 1 ml of 10% acetic acid, boiled for 5 min, and filtered in a centricon 3 (molecular weight cutoff of 3,000) ultrafiltration device. The filtrates were analyzed on a SMART system μRPC C2/C18 SC column using a 6 ml gradient from 0.06% trifluoroacetic acid in water to 0.05% trifluoroacetic acid in 80% acetonitrile. Absorbance was monitored at 214 nm. The fractions containing peaks were microsequenced using an ABI 477A protein sequencer with a 120A phenyl-thiohydantoin analyzer as described (4). To detect N-terminally blocked peptides, peaks from a similar experiment were analyzed by matrix-assisted, laser desorption, time-of-flight mass spectrometry using a PerSeptive Biosystems (Framingham, MA) ELITE mass spectrometer.

Thermal Stability Analyses. An Aviv 62A DS spectropolarimeter equipped with a thermoelectric cell holder and a 1-mm path-length cell was used for CD studies. The heat-induced unfolding of ZAG [1 mg/ml in 5 mM sodium phosphate (pH 7)] was monitored by recording the CD signal at 223 nm while the sample temperature was raised from 25° to 80°C at a rate of 20°C per hour. The transition midpoint (T_m) was calculated by estimating the half-point of the ellipticity change between the pure native and the pure denatured states. Thermal stability measurements were repeated after denaturation in 6 M guanidine hydrochloride, dialysis against denaturant, and refolding by dialysis against 5 mM sodium phosphate (pH 7).

Crystalization of ZAG. Initial crystalization conditions were obtained from factorial trial screens (23). The best crystals were obtained using serum ZAG eluted with 0.56 M $(NH_4)_2SO_4$ from the Source phenyl column. Single crystals were grown by vapor diffusion from protein solutions (15 mg/ml) in 20 mM Hepes (pH 7.0), 0.02% NaN_3, in 3-μl droplets with 30% (wt/vol) polyethylene glycol 2000 monomethyl ether (Fluka), 0.2 M ammonium acetate, 0.1 M sodium acetate (pH 5). After crystals were formed, the concentration of polyethylene glycol was raised to 35% for cryopreservation. Single crystals were mounted in a thin film of cryopreservation buffer, supported by a rayon loop (24), and quickly cooled by plunging into liquid nitrogen.

RESULTS

Purification of ZAG. High levels of ZAG are found in the fluid from breast cysts obtained from patients with breast gross cystic disease (4). We developed a purification protocol for isolation of ZAG from breast cyst fluid, which yielded about 20 mg of ZAG per 75 ml of fluid. The purification procedure included three successive chromatographic steps: hydrophobic interaction, metal chelating, and size exclusion chromatogra-

phy, and resulted in protein that was apparently homogeneous, as judged by SDS/PAGE (Fig. 1). However, subsequent analysis by native PAGE (Fig. 1) revealed heterogeneity in the protein preparation, and multiple crystalization trials failed to produce protein crystals of x-ray diffraction quality. We therefore decided to purify ZAG from another source.

To facilitate purification of ZAG from human serum, mAbs were produced against ZAG purified from breast cyst fluid. The anti-ZAG mAb 3C5 was immobilized on a solid support, and ZAG was purified by immunoaffinity and ion exchange chromatography from serum at yields up to 15 mg/liter. SDS/PAGE (Fig. 1) and mass spectrometry showed that both serum and cyst fluid ZAG have the same molecular mass (39 ± 1 kDa by mass spectrometry; data not shown). However, native PAGE analysis revealed that ZAG isolated from serum was more homogeneous than ZAG isolated from cyst fluid (Fig. 1). Therefore, serum ZAG was used for the subsequent experiments.

β_2m Binding Assays. The heavy chains of classical class I MHC proteins are tightly associated with β_2m (25). However, purified preparations of ZAG show a single band with an apparent molecular mass of 41 kDa when analyzed by SDS/PAGE, with no sign of a 12-kDa light chain corresponding to β_2m (Fig. 1). To ascertain if ZAG binds β_2m, different ratios of both proteins were incubated and analyzed by size exclusion chromatography. Regardless of the ZAG/β_2m ratio loaded on the column, only peaks containing either ZAG or β_2m, but not both proteins, were obtained (Fig. 2A). In addition, β_2m binding was not observed using a surface plasmon resonance-based assay in which β_2m was passed over a ZAG-coupled biosensor chip (data not shown).

The result that purified ZAG does not associate with β_2m was confirmed for ZAG in serum using immunoprecipitation assays. Western blot analysis showed that an anti-ZAG antiserum precipitated ZAG from serum, but did not coprecipitate β_2m. Conversely, an anti-β_2m antiserum precipitated β_2m from serum, but did not coprecipitate ZAG (Fig. 2B).

Peptide Elution Assays. Peptides associated with class I MHC molecules have typically been analyzed by N-terminal sequencing of eluates recovered after ultrafiltration of acid dissociated heterodimers (21, 22). To determine whether ZAG contains bound peptide(s), we compared acid eluates of purified ZAG and the murine class I MHC molecule H-2K^d. Acid eluates were analyzed by reverse phase chromatography (Fig. 3) and N-terminal sequencing. This procedure resulted in identification of multiple peptides in the K^d acid eluate whose sequences corresponded to the previously characterized motif for peptides bound to this class I allele (26). By contrast, most of the peaks in the chromatographic profile of the ZAG acid eluate also were found in eluates extracted from samples without protein, and peptides were not detected in any of the
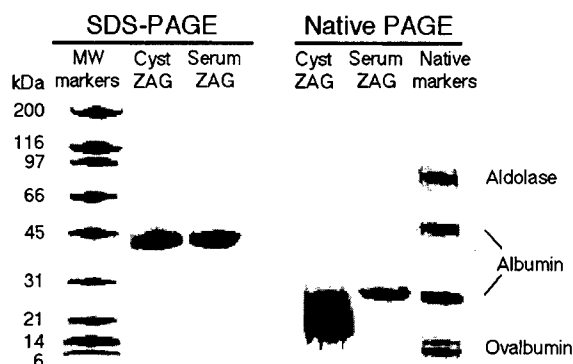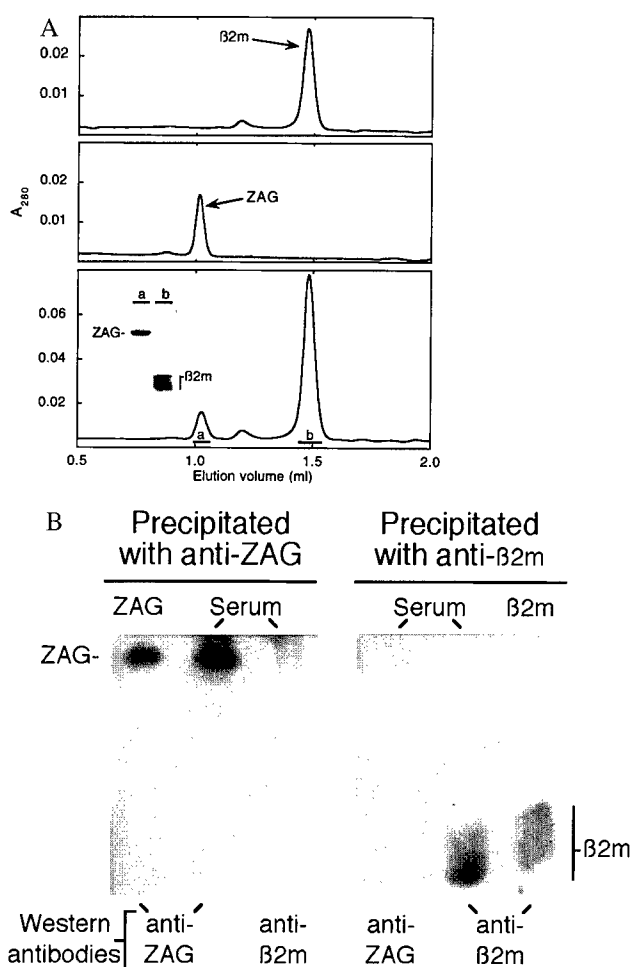

FIG. 2. Chromatographic and immunoprecipitation analyses confirm that ZAG does not bind β_2m. (*A*) β_2m (*Top*), ZAG (*Middle*), and a mixture of ZAG incubated with β_2m (*Bottom*) were analyzed by size exclusion chromatography. (*Inset*) SDS/13% PAGE analysis of the peaks in the bottom panel. (*B*) Aliquots of ZAG, serum, and β_2m were immunoprecipitated with either anti-ZAG or anti-β_2m antibodies. Precipitated proteins were analyzed by Western blot using antisera against either ZAG or β_2m.

peaks by N-terminal sequencing or by mass spectrometry. Pool sequencing of unpurified acid eluates produced comparable results: peptides were detected in the K^d eluate, but not in the ZAG eluate (data not shown).

Thermal Stability of ZAG. Class I MHC heavy chains show decreased stability in the absence of peptide (20, 27, 28) or β_2m (29), whereas ZAG exists as an isolated class I MHC-like heavy chain without bound peptides. To ascertain if ZAG is less stable than class I MHC molecules because of the absence of bound peptide and light chain, we monitored the heat-induced unfolding of ZAG by recording the CD signal at 223 nm while increasing the sample temperature from 25°C to 80°C (Fig. 4). The resulting melting curve shows a T_m of 65°C, which is comparable to previously obtained T_ms for peptide-filled class I MHC molecules [H-2K^d: 57°C; (20); HLA-A2: 66°C; (30)]. The T_m obtained from the ZAG melting curve is substantially higher than the T_m of an empty class I MHC molecule (H-2K^d complexed with human or murine β_2m: 43–45°C; refs. 20 and 31).

Crystalization. ZAG forms crystals of approximate dimensions 0.4 mm × 0.2 mm × 0.1 mm in space group $P2_12_12$. The unit cell dimensions are $a = 106$ Å, $b = 132$ Å, and $c = 119$ Å. The asymmetric unit of the crystal is estimated to contain two to six molecules based on average volume to mass ratios

FIG. 1. PAGE analysis of ZAG. Aliquots of ZAG purified from breast cyst fluid or serum were analyzed by SDS/10–15% PAGE and native/8–20% PAGE.
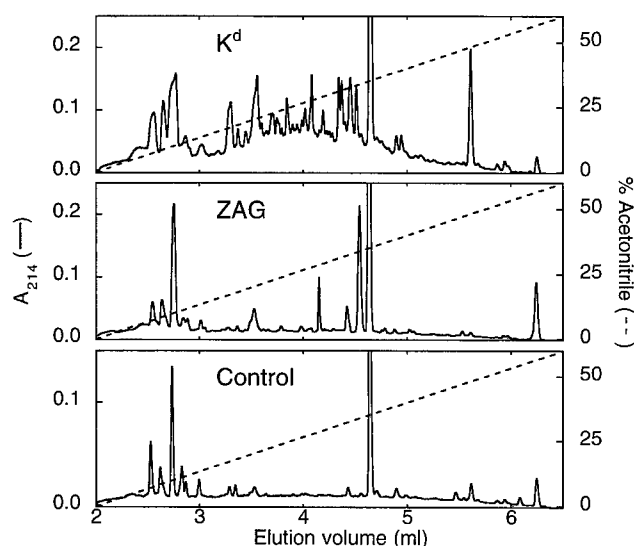
FIG. 3.   HPLC analysis of acid eluates from K^d, ZAG, and a control with no protein. All peaks in the ZAG eluate were subjected to N-terminal sequencing and mass spectrometry analysis. No peptides were detected.

(V_m) of protein crystals (32), representing solvents contents between 76% (assuming two molecules per asymmetic unit) to 27% (assuming six molecules per asymmetric unit). Crystals were equilibrated in a cryopreservative and subjected to x-ray analysis at −165°C (33). Cryopreserved crystals diffract to 3.2 Å resolution using CuKα radiation from a Rigaku R200 rotating anode x-ray generator. The use of a synchrotron x-ray source improves the resolution limit. Using the A1 beam line at the Cornell High Energy Synchrotron Source (CHESS), data were collected to 2.7 Å resolution from cryopreserved crystals. We are in the process of solving the three-dimensional structure of ZAG using molecular and isomorphous replacement methods.
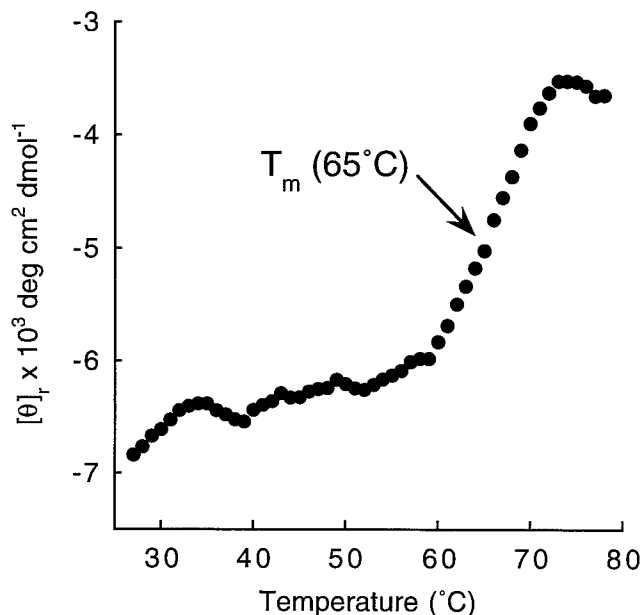

FIG. 4.   Thermal denaturation profile of serum ZAG. The CD signal at 223 nm is plotted as molar ellipticity per mean residue after smoothing. Similar profiles were obtained using ZAG isolated from cyst fluid. Thermal denaturation studies were repeated after denaturation and dialysis to remove any potential ZAG ligands without any effect on the denaturation profile.

DISCUSSION

ZAG is a class I MHC homolog produced by secretory epithelial cells that is present in most bodily fluids (2). Because of increased concentrations of ZAG in mammary carcinomas and in cyst fluids from women with gross cystic disease of the breast, it has been suggested that ZAG participates in the development of breast diseases (4). Indeed, ZAG levels are higher in well differentiated breast carcinomas, indicating that ZAG is a biochemical marker of differentiation in breast cancer (5). In this study, we have purified human ZAG from both breast cyst fluids and serum, and compared a series of biochemical characteristics to those of class I MHC molecules. Milligram amounts of ZAG were purified from cyst fluid obtained from women with breast gross cystic disease and used for production of mAbs. These mAbs are suitable for detection of ZAG by immunoprecipitation and Western blot analyses, and may serve as useful reagents for clinical evaluation of ZAG as a biochemical marker of tumors with specific patterns of hormone responsiveness (5, 7). Our inability to produce crystals of ZAG purified from cyst fluid prompted us to isolate ZAG from serum using one of the anti-ZAG mAbs for immunoaffinity chromatography. Additional chromatographic steps resulted in fractionation of ZAG into different forms, one of which yielded well ordered crystals.

ZAG purified from serum and cyst fluid consists of a single chain, by contrast to the related class I MHC molecules, which are heterodimers consisting of a membrane-bound heavy chain associated with $\beta_2 m$, a soluble light chain. To investigate whether ZAG is capable of binding the class I light chain, we incubated purified ZAG with human $\beta_2 m$. No sign of a ZAG/$\beta_2 m$ heterodimer was observed by size exclusion chromatography. In addition, immunoprecipitation studies using antibodies against either ZAG or $\beta_2 m$ showed that the two proteins do not coprecipitate from human serum. Therefore, unlike most classical and nonclassical class I MHC proteins, ZAG is not associated with the class I light chain, a characteristic it shares with MICA, a divergent member of the class I MHC family (34).

Class I MHC molecules require bound peptide for structural stability (20, 27, 28). Although ZAG is secreted from cells, differing from conventional class I MHC molecules and most MHC homologs which are cell surface proteins, soluble versions of H-2K^d (20) and HLA-G (35) have been shown to bind peptides derived from endogenous proteins. We therefore examined purified ZAG for the presence of bound peptide. Peptides were not detected in acid eluates derived from ZAG, by contrast to results obtained with the K^d eluate. To ascertain if ZAG is stably folded in the absence of bound peptide and $\beta_2 m$, we compared the thermal denaturation profile of ZAG with denaturation profiles of class I molecules. The CD-monitored melting curve of purified ZAG indicated that this protein is significantly more stable than empty class I molecules (20), and as stable as peptide-filled class I MHC heterodimers (20, 30). The structural stability in the absence of peptide or $\beta_2 m$ binding indicates that the function of ZAG has diverged from the peptide presentation and T cell interaction functions of class I MHC molecules and seems to rule out the previous suggestion that ZAG functions as a soluble MHC protein to regulate the immune system (8). Several lines of evidence suggest that ZAG is a carrier of a small molecular mass compound. When the protein was originally isolated from serum, it was noted that ZAG was bound to a yellow pigment that could be removed upon denaturation (1), and we have obtained similar results with ZAG isolated from breast cyst fluid (L.M.S. and C.L.-O., unpublished results). Moreover, immunological studies showed that ZAG carries a proteinase-resistant, heat-stable substance whose injection induces glomerulonephritis in experimental animals (36). Taken together, these data suggest that ZAG carries a low molecular mass

ligand of a different chemical nature than the peptides bound by MHC molecules, but further studies will be needed to identify the nature of the ZAG ligand(s).

Class I MHC molecules acquire peptide during assembly of their heavy and light chains in the endoplasmic reticulum (9). Because ZAG follows the same biosynthetic pathway as class I molecules, it has an opportunity to bind peptides in the endoplasmic reticulum, yet the biochemical data reported here show that it does not. The neonatal Fc receptor (FcRn) is another class I MHC homolog that does not bind endogenous peptides (37). The FcRn crystal structure reveals that the FcRn counterpart of the MHC peptide binding groove is closed (38), resulting in an MHC-like structure that is stable in the absence of bound peptide (37). Two amino acid changes with respect to MHC molecules are primarily responsible for closure of the FcRn cleft: Arg-164 occludes the FcRn counterpart of pocket A that is used by class I molecules for the peptide N terminus (reviewed in ref. 11), and Pro-162 within the α_2 domain helix appears to be responsible for a kink that closes one side of the cleft. Interestingly, ZAG is one of only a few MHC-like molecules that contains a proline at the position of FcRn Pro-162 (Pro-167 in mature ZAG; classical human and murine class I molecules contain mainly valine, a helix-forming residue, at this position). In addition to ZAG and FcRn, proline is found at the analogous position in all CD1 sequences (39). The recent crystal structure of a murine CD1 molecule shows a kink in the α_2 domain helix at the position of its proline, and some of the same sort of underlying structural changes that were seen in the FcRn structure (40). At least one form of human CD1 binds lipids instead of peptide antigens (41, 42), and the murine CD1 structure shows a substantially deeper and more hydrophobic binding groove than conventional class I molecules (40). The available structural evidence, therefore, suggests that a proline at this position within the α_2 domain helix could be indicative of a structural rearrangement with respect to classical class I MHC molecules, which might be predictive of a function other than peptide binding. X-ray structural analysis of ZAG ultimately should allow its comparison with MHC and MHC-related molecules, and increase understanding of the function of ZAG under physiological and cancerous conditions.

1. Bürgi, W. & Schmid, K. (1961) *J. Biol. Chem.* **236**, 1066–1074.
2. Tada, T., Ohkubo, I., Niwa, M., Sasaki, M., Tateyama, H. & Eimoto, T. (1991) *J. Histochem. Cytochem.* **39**, 1221–1226.
3. Bundred, N. J., Miller, V. R. & Walker, R. A. (1987) *Histopathology* **11**, 603–610.
4. Sánchez, L. M., Vizoso, F., Diez-Itza, I. & López-Otín, C. (1992) *Cancer Res.* **52**, 95–100.
5. Díez-Itza, I., Sánchez, L. M., Allende, M. T., Vizoso, F., Ruibal, A. & López-Otín, C. (1993) *Eur. J. Cancer* **29**, 1256–1260.
6. Freije, J. P., Fueyo, A., Uría, J. & López-Otín, C. (1991) *FEBS Lett.* **290**, 247–249.
7. López-Boado, Y., Diez-Itza, I., Tolivia, J. & López-Otín, C. (1994) *Breast Cancer Res. Treat.* **29**, 247–258.
8. Araki, T., Gejyo, F., Takagaki, K., Haupt, H., Schwick, H. G., Bürgi, W., Marti, T., Schaller, J., Rickli, E., Brossmer, R., Atkinson, P. H., Putnam, F. W. & Schmid, K. (1988) *Proc. Natl. Acad. Sci. USA* **85**, 679–683.
9. Townsend, A. & Bodmer, H. (1989) *Annu. Rev. Immunol.* **7**, 601–624.
10. Bjorkman, P. J. & Parham, P. (1990) *Annu. Rev. Biochem.* **90**, 253–88.
11. Stern, L. J. & Wiley, D. C. (1994) *Structure* **15**, 245–251.
12. Chothia, C. & Lesk, A. M. (1986) *EMBO J.* **5**, 823–826.
13. Freije, J. P., Fueyo, A., Uría, J. A., Velasco, G., Sánchez, L. M., López-Boado, Y. S. & López-Otín, C. (1993) *Genomics* **18**, 575–587.
14. Pendas, A. M., Matilla, T., Uría, J. A., Freije, J. P., Fueyo, A., Estivill, X. & López-Otin, C. (1994) *Cytogenet. Cell Genet.* **64**, 263–266.
15. Fueyo, A., Uría, J. A., Freije, J. M. P. & López-Otin, C. (1994) *Gene* **145**, 245–249.
16. Ueyama, H., Naitoh, H. & Ohkubo, I. (1994) *J. Biochem.* **116**, 677–681.
17. Li, W.-H., Gouy, M., Sharp, P. M., O'Huigin, C. & Yang, Y.-W. (1990) *Proc. Natl. Acad. Sci. USA* **87**, 6703–6707.
18. Raghavan, M., Chen, M. Y., Gastinel, L. N. & Bjorkman, P. J. (1994) *Immunity* **1**, 303–315.
19. Pepper, D. S. (1992) in *Methods in Molecular Biology*, eds. Kenney, A. & Fowell, S. (Humana Press, Totowa, NJ), Vol. 11, pp. 135–171.
20. Fahnestock, M. L., Tamir, I., Narhi, L. & Bjorkman, P. J. (1992) *Science* **258**, 1658–1662.
21. Van Bleek, G. M. & Nathenson, S. G. (1990) *Nature (London)* **348**, 213–216.
22. Jardetzky, T. S., Lane, W. S., Robinson, R. A., Madden, D. R. & Wiley, D. C. (1991) *Nature (London)* **353**, 325–330.
23. Jancarik, J. & Kim, S. H. (1991) *J. Appl. Cryst.* **24**, 409–411.
24. Teng, T.-Y. (1990) *J. Appl. Cryst.* **23**, 387–391.
25. Grey, M. M., Kubo, R. T., Colon, S. M., Poulik, M. D., Cresswell, P., Springer, T. A., Turner, M. & Strominger, L. (1973) *J. Exp. Med.* **138**, 1608–1612.
26. Falk, K., Rötzschke, O., Stevanovic, S., Jung, G. & Rammensee, H. G. (1991) *Nature (London)* **351**, 290–296.
27. Townsend, A., Elliott, T., Cerundolo, V., Foster, L., Barber, B. & Tse, A. (1990) *Cell* **62**, 285–295.
28. Ljunggren, H. G., Stam, N. J., Öhlén, C., Neefjes, J. J., Höglund, P., Heemels, M. T., Bastin, J., Schumacher, T. N. M., Townsend, A., Kärre, K. & Ploegh, H. L. (1990) *Nature (London)* **346**, 476–480.
29. Lancet, D., Parham, P. & Strominger, J. L. (1979) *Proc. Natl. Acad. Sci. USA* **76**, 3844–3848.
30. Bouvier, M. & Wiley, D. C. (1994) *Science* **265**, 398–402.
31. Fahnestock, M. L., Johnson, J. L., Feldman, R. M. R., Tsomides, T. J., Mayer, J., Narhi, L. O. & Bjorkman, P. J. (1994) *Biochemistry* **33**, 8149–8158.
32. Matthews, B. W. (1968) *J. Mol. Biol.* **33**, 491–497.
33. Hope, H. (1990) *Annu. Rev. Biophys. Biophys. Chem.* **19**, 107–126.
34. Groh, V., Bahram, S., Bauer, S., Herman, A., Beauchamp, M. & Spies, T. (1996) *Proc. Natl. Acad. Sci. USA* **93**, 12445–12450.
35. Lee, N., Malacko, A. R., Ishitani, A., Chen, M. C., Bajorath, J., Marquardt, H. & Geraghty, D. E. (1995) *Immunity* **3**, 591–600.
36. Shibata, S. & Miura, K. (1982) *Nephron* **31**, 170–176.
37. Raghavan, M., Gastinel, L. N. & Bjorkman, P. J. (1993) *Biochemistry* **32**, 8654–8660.
38. Burmeister, W. P., Gastinel, L. N., Simister, N. E., Blum, M. L. & Bjorkman, P. J. (1994) *Nature (London)* **372**, 336–343.
39. Martin, L. H., Calabi, F., Lefevre, F.-A., Bilsland, C. A. & Milstein, C. (1987) *Proc. Natl. Acad. Sci. USA* **84**, 9189–9193.
40. Zeng, Z. H., Castaño, A. R., Segelke, B., Stura, E. A., Peterson, P. A. & Wilson, I. A. (1997) *Science*, in press.
41. Beekman, E. M., Porcelli, S. A., Morita, C. T., Behar, S. M., Furlong, S. T. & Brenner, M. B. (1994) *Nature (London)* **372**, 691–694.
42. Sieling, P. A., Chatterjee, D., Porcelli, S. A., Prigozy, T. I., Mazzaccaro, R. J., Soriano, T., Bloom, B. R., Brenner, M. B., Kronenberg, M., Brennan, P. J. & Modlin, R. L. (1995) *Science* **269**, 227–230.

Crystal Structure of Human
ZAG, a Fat-Depleting Factor
Related to MHC Molecules

Luis M. Sánchez,[1]* Arthur J. Chirino,[1,2]* and Pamela J. Bjorkman[1,2]†

Crystal Structure of Human ZAG, a Fat-Depleting Factor Related to MHC Molecules

Luis M. Sánchez,[1]* Arthur J. Chirino,[1,2]* Pamela J. Bjorkman[1,2]†

Zn-α_2-glycoprotein (ZAG) is a soluble protein that is present in serum and other body fluids. ZAG stimulates lipid degradation in adipocytes and causes the extensive fat losses associated with some advanced cancers. The 2.8 angstrom crystal structure of ZAG resembles a class I major histocompatibility complex (MHC) heavy chain, but ZAG does not bind the class I light chain β_2-microglobulin. The ZAG structure includes a large groove analogous to class I MHC peptide binding grooves. Instead of a peptide, the ZAG groove contains a nonpeptidic compound that may be implicated in lipid catabolism under normal or pathological conditions.

ZAG is a soluble protein whose name derives from its tendency to precipitate with zinc salts and its electrophoretic mobility in the region of the α_2 globulins (*1*). ZAG is normally present in most body fluids including serum, sweat, saliva, cerebrospinal fluid, seminal plasma, milk, amniotic fluid, and urine (*1*). In addition, ZAG accumulates in breast cysts as well as in 40% of breast carcinomas, and is induced by glucocorticoids and androgens in breast cancer cell lines. Hence, ZAG may participate in breast diseases, including cancer (*2*).

The function of ZAG was elucidated when a lipid-catabolizing factor with the same amino acid sequence as ZAG was isolated from the urine of cancer patients with cachexia (*3*). Cachexia is a wasting syndrome caused by depletion of muscle and adipose tissue that is present in the majority of patients with cancer, AIDS, and other life-threatening diseases (*3*). ZAG appears to be responsible for the fat-depletion component of cachexia, since it stimulates lipid breakdown in adipocytes and reduces fat stores in laboratory animals (*3*). ZAG is overexpressed in carcinomas that induce fat loss but not in other tumors. Application of ZAG to adipocyte membranes activates a guanosine triphosphate–dependent adenylate cyclase ac-

tivity, perhaps through direct or indirect interactions with a G protein–coupled receptor (*3*). Thus, its mode of action could be similar to that of lipolytic hormones. These results suggest that ZAG normally functions to regulate lipid degradation, which increases to a pathological extent in cachexia.

ZAG shares 30 to 40% amino acid sequence identity with the extracellular portions of class I major histocompatibility complex (MHC) heavy chains (*4*). Class I MHC molecules present peptide antigens to cytotoxic T cells (*5*). Other proteins related to class I MHC molecules include CD1, which presents hydrophobic antigens to T cells (*6*), the neonatal Fc receptor (FcRn), which transports immunoglobulin G across epithelia (*7*), and HFE, which binds transferrin receptor and regulates iron homeostasis (*8*). These MHC homologs are membrane-bound heterodimers that use the soluble protein β_2-microglobulin (β_2M) as a light chain. ZAG, however, is a secreted protein, and it does not associate with β_2M (*9*). The latter property is shared by MIC-A, a divergent membrane-bound member of the class I family (*10*).

Like FcRn (*11*), HFE (*11*), and MIC-A (*10*), ZAG does not bind endogenous peptides (*9*), but it appears to carry a small proteinase-resistant compound whose injection induces glomerulonephritis in experimental animals (*12*). In peptide-binding class I MHC molecules, a large groove located between two α helices in the $\alpha1$-$\alpha2$ superdomain of the heavy chain serves as the binding site (*5*). An analogous groove acts as the antigen binding site in CD1,

[1]Division of Biology 156-29 and [2]Howard Hughes Medical Institute, California Institute of Technology, Pasadena, CA 91125, USA.

*These authors contributed equally to this work.
†To whom correspondence should be addressed. E-mail: bjorkman@cco.caltech.edu

but is narrowed in HFE and closed in FcRn, the class I–related proteins that do not bind small molecular weight ligands (*11*).

Here, we present the 2.8 Å crystal structure of human ZAG, which reveals an MHC-like fold without a β_2M light chain and a groove that closely resembles the peptide-binding sites of classical class I MHC molecules. Rather than containing a peptide, the
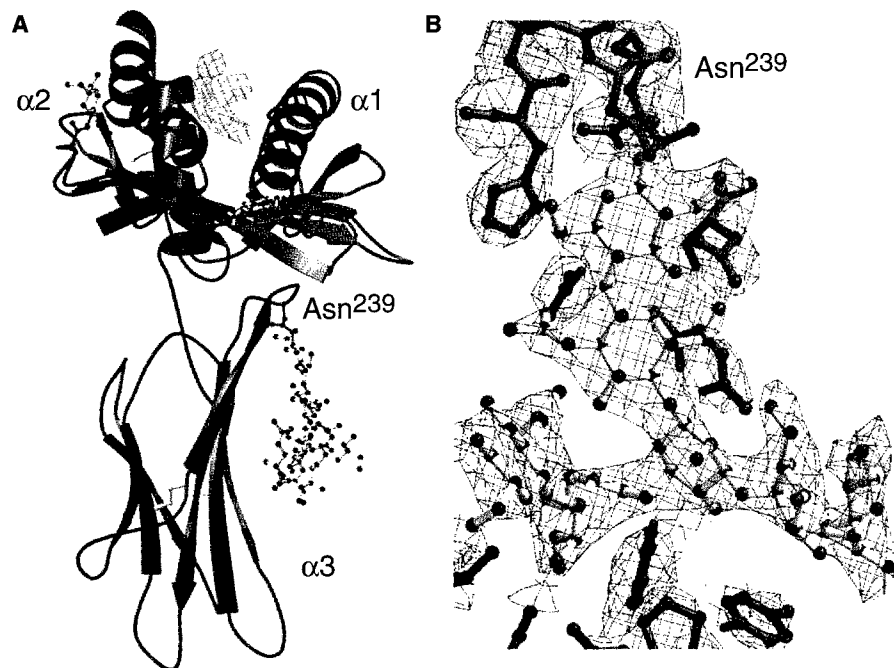

Fig. 1. (A) Ribbon diagram of the structure of human ZAG. Density corresponding to the non-peptidic ligand is shown in green as derived from a 2.9 Å MIRAS, NCS averaged, figure-of-merit weighted electron density map contoured at 1σ. Ordered N-linked carbohydrates are shown in ball-and-stick representation. **(B)** The ZAG model (molecule 2) in the region of the N-linked carbohydrate attached to Asn[239] superimposed on a 2.8 Å SIGMAA-weighted $2F_o - F_c$ annealed omit electron density map (*13*). The carbohydrate electron density at Asn[239] shows nine carbohydrate residues arranged in a biantennary structure (*14*) (two of the carbohydrate residues are omitted from the figure for clarity). The large number of ordered carbohydrate residues at Asn[239] is likely to result from stabilization of the flexible carbohydrate by crystal contacts with protein residues in symmetry-related ZAG molecules (shown in red sticks; bottom). Figures were made as described (*23*).

Table 1. Data collection, heavy-atom phasing, and refinement statistics for ZAG. Statistics in parentheses refer to the highest resolution bin. ZAG was crystallized in space group P2₁2₁2 with four molecules per asymmetric unit and cryoprotected as described (*9*). Native and heavy-atom derivative data sets were collected at −165°C from multiple crystals using an R-AXIS IIc imaging plate system mounted on a Rigaku R200 rotating anode generator.

Data were processed and scaled with the HKL package (*13*). Heavy-atom refinement was done with SHARP (*13*), which treated different data sets of derivatives with the same sites as separate "crystals" of the same "compound" and refined separate heavy-atom occupancies and temperature factors for each "crystal" data set. Electron density maps calculated from MIRAS phases derived from all eight heavy-atom data sets were superior to maps derived from various combinations of mercury and platinum data sets. Eight NCS operators were determined from least squares superposition of HLA-A2 α1-α2 and α3 domains manually placed in the electron density, four relating the α1-α2 regions and four relating the α3 domains. After solvent flipping using Solomon (*13*), subdomain NCS averaging of the four molecules and phase extension from 5.0 to 2.9 Å were carried out with DM in the CCP4 suite (*13*) (final average correlation >0.8). When the same averaging and phase extension procedure was done without prior solvent flipping, the resulting electron density maps were inferior. The model was built using O (*13*) and refined as described (*13*).

Data set	Resolution (Å)	Complete (%)*	R_{merge}(%)†	I/σI	rms f_h/E‡
Native I	2.9	97.0 (83.0)	10.7 (29.7)	27.9 (3.2)	
Native II	2.8	96.0 (76.0)	6.6 (45.3)	24.7 (2.5)	
Mercury acetate					
1	3.4	94.4 (97.5)	13.6 (30.4)	10.8 (4.4)	3.0
2	4.0	94.4 (97.2)	17.9 (35.5)	6.8 (3.3)	2.2
3	3.4	98.5 (99.1)	13.2 (32.4)	9.9 (3.9)	2.8
4	3.2	97.7 (93.3)	7.8 (30.8)	19.1 (4.3)	1.9
PIP§					
1	3.7	91.8 (77.3)	5.7 (35.4)	22.1 (3.5)	1.1
2	3.2	98.5 (97.7)	7.3 (33.6)	22.0 (4.1)	0.8
3	3.6	95.4 (96.4)	8.1 (29.5)	20.8 (5.2)	1.0
K₂PtCl₄	4.0	98.8 (99.3)	13.0 (39.5)	10.1 (3.1)	1.5

Refinement statistics				
Resolution (Å)		20.0–2.8	rms ΔB bonded NCS atoms (Å²)#	14.4, 15.4, 19.0
Reflections in working set	$|F| > 0$	37148	rms Δφ all NCS residues (degrees)#	2.4, 3.2, 3.7
Reflections in test set	$|F| > 0$	1970	rms Δψ all NCS residues (degrees)#	2.0, 2.3, 2.4
R_{free} (%) ‖		28.8		
R_{cryst} (%) ¶		22.9	Number of nonhydrogen atoms	
rms deviations from ideal			Protein	8866
Bond lengths (Å)		0.008	Carbohydrate	388
Bond angles (degrees)		1.35	Nonglycine residues in allowed regions of Ramachandran plot as defined (*13*)	96%

*Complete = (number of independent reflections)/total theoretical number. †R_{merge} (I) = $[\Sigma|I(i) - \langle I(h)\rangle|/\Sigma I(i)]$, where I(i) is the *i*th observation of the intensity of the hkl reflection and ⟨I⟩ is the mean intensity from multiple measurements of the hkl reflection. ‡rms f_h/E (phasing power), where f_h is the heavy-atom structure factor amplitude and E is the residual lack of closure error. §PIP, di-m-iodobis(ethylenediamine)diplatinum nitrate. ‖R_{free} is calculated over reflections in a test set not included in atomic refinement. ¶R_{cryst} (F) = $\Sigma_h||F_{obs}(h)| - |F_{calc}(h)||/\Sigma_h|F_{obs}(h)|$, where $|F_{obs}(h)|$ and $|F_{calc}(h)|$ are the observed and calculated structure factor amplitudes for the hkl reflection. #Statistics for NCS-related residues refer to differences relative to molecule 1 for the other three molecules in the crystallographic asymmetric unit.

ZAG groove includes an unidentified non-peptidic ligand that may be relevant for ZAG's function in lipid catabolism.

ZAG was purified from human serum and crystallized as described (9). The crystal structure was determined by multiple isomorphous replacement with anomalous scattering (MIRAS) aided by fourfold noncrystallographic symmetry (NCS) averaging (Table 1) (13). The overall structure of ZAG is similar to those of class I MHC heavy chains (Fig. 1A). The α1-α2 superdomains of ZAG, class I, and class I–related proteins form a single eight-stranded antiparallel β sheet topped by two α helices, and the α3 domain adopts a fold resembling immunoglobulin constant domains (5, 11). Electron density corresponding to carbohydrate is present at three of the four potential N-linked glycosylation sites in ZAG, with an unusually large number of ordered carbohydrate residues visible at Asn[239] (Fig. 1B) (14). The α3 domain of human, but not mouse or rat, ZAG contains an RGD sequence (Arg[231], Gly[232], Asp[233]) suggested to be involved in cell adhesion (15). However, unlike the RGD sequences in characterized adhesion molecules such as fibronectin III domains (15), the ZAG RGD is located in a β strand rather than a loop.

The quaternary arrangement of the ZAG α3 domain with respect to the α1-α2 platform differs from that found in β2M-binding class I and class I–related proteins. The overall shape of ZAG is similar to an inverted "L," in which the long axis of the α3 domain is roughly perpendicular to the flat side of the α1-α2 platform, whereas the comparable angle is acute in β2M-binding proteins (Fig. 2A). In those proteins, β2M interacts with the α3 domain and the underside of the α1-α2 platform and is typically required for stability (16). The displacement of the ZAG α3 domain compared to its class I counterpart results in the inability of β2M to optimally contact the α3 and α1-α2 domains of ZAG (17), contributing to ZAG's lack of affinity for β2M. The high thermal stability of ZAG in the absence of β2M (9) can be explained by a network of hydrogen bonds between α3 and α1-α2 that are not present in β2M-binding class I proteins (Fig. 2B). In addition to the extra hydrogen bonds, the loop connecting β strand 4 to the helical region of the ZAG α1 domain platform (residues 51 to 54) and the loop connecting strands D to E in the α3 domain (residues 236 to 241) are closer together than their class I counterparts, contributing to the burial of a larger interdomain surface in ZAG (970 Å² total) than in classical class I molecules (660 Å² in HLA-A2) (11). There is some flexibility in the position of the ZAG α3 domain relative to α1-α2, as demonstrated by different interdomain relationships of the four ZAG molecules in the crystallographic asymmetric unit (Fig. 2A), yet ZAG is not particularly protease-sensitive at the platform-
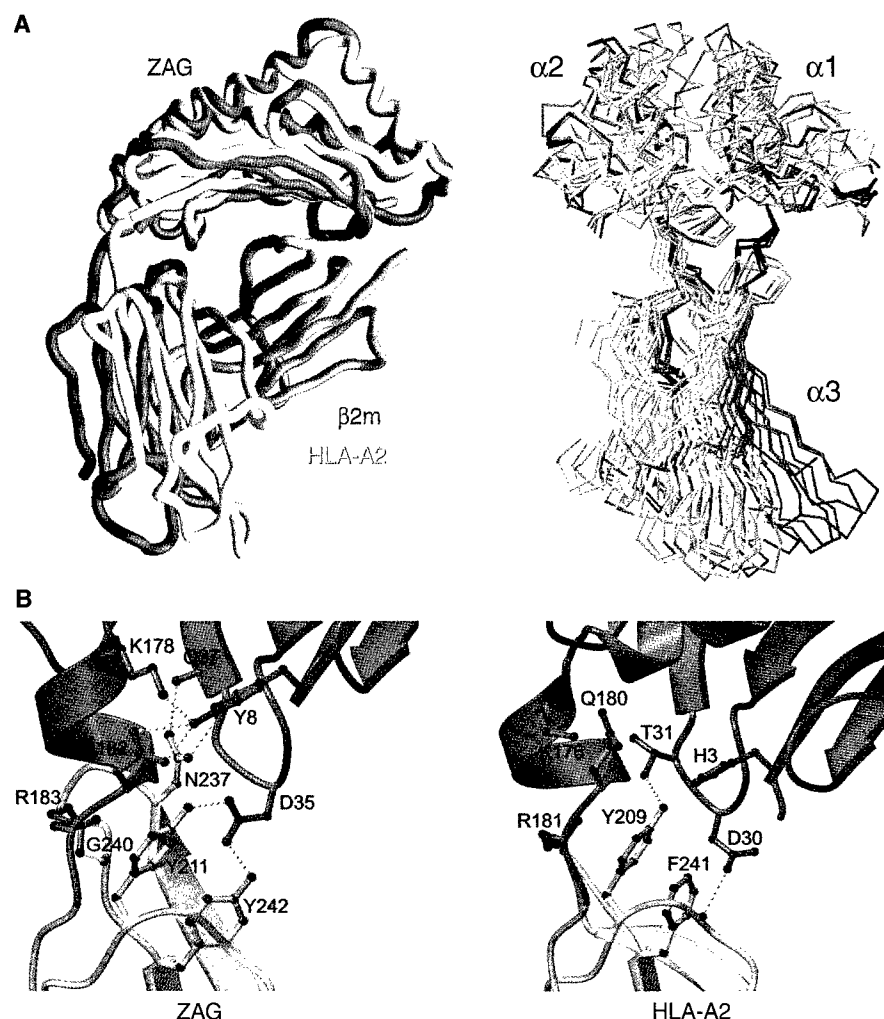

Fig. 2. Structural comparisons of ZAG, class I, and class I–related proteins. (A) (Left) Comparison of the structures of ZAG and HLA-A2 (11). (Right) Comparison of the four ZAG molecules in the crystallographic asymmetric unit (magenta) with the heavy chains of human class I MHC (yellow; PDB codes 1hhh, 1vac, 2clr) and β2M-binding class I MHC homologs (green; FcRn, CD1, HFE) (11). Superpositions were based on the Cα atoms in the platform domains, using 2clr as a reference molecule. The position of the ZAG α3 domain with respect to its α1-α2 platform falls out of the range of the positions of the α3 domains of the β2M-binding class I proteins. Differences in the platform-α3 interdomain relationships in the four ZAG molecules demonstrate that there is flexibility in the position of the ZAG α3 domain relative to α1-α2. However, the overall similarity of the four molecules, which are subjected to different crystal packing forces, rule out that ZAG's shape is an artifact of crystallization. (B) Close-up comparison of the interface between α1-α2 (blue) and α3 (green) in ZAG and HLA-A2 (11). Additional H-bonds and a larger interdomain surface area stabilize ZAG compared with class I molecules, whose heavy chains are stabilized by interactions with β2M. Figures were made as described (23).

α3 hinge or any other region (18). Although the quaternary structure of ZAG differs significantly from the heavy chains of class I and class I-like structures, the differences are less than anticipated from the absence of the β2M light chain. The overall similarity between ZAG and class I MHC heavy chains contrasts with the large interdomain rearrangements observed in the crystal structure of MIC-A (10).

Despite the similarity between ZAG and class I molecules, structural features of the ZAG α3 domain make it unlikely to associate with the T cell coreceptor CD8. Of 15 class I heavy-chain residues identified at the CD8 binding site in the HLA-A2/CD8 cocrystal

structure (19), only one is conserved between class I and ZAG sequences (class I Asp[122], ZAG Asp[123]) (4). It is not possible to rule out an interaction between ZAG and T cell receptors, because the class I MHC residues that contact these receptors are not particularly conserved (20).

Although ZAG does not associate with peptides (9), the helices in both the α1 and α2 domains are almost identically positioned to their counterparts in peptide-binding class I MHC molecules (Fig. 3A) (21). Thus, the ZAG platform includes an open groove, by contrast to the narrowed or closed grooves observed in other class I homologs that do not bind peptides
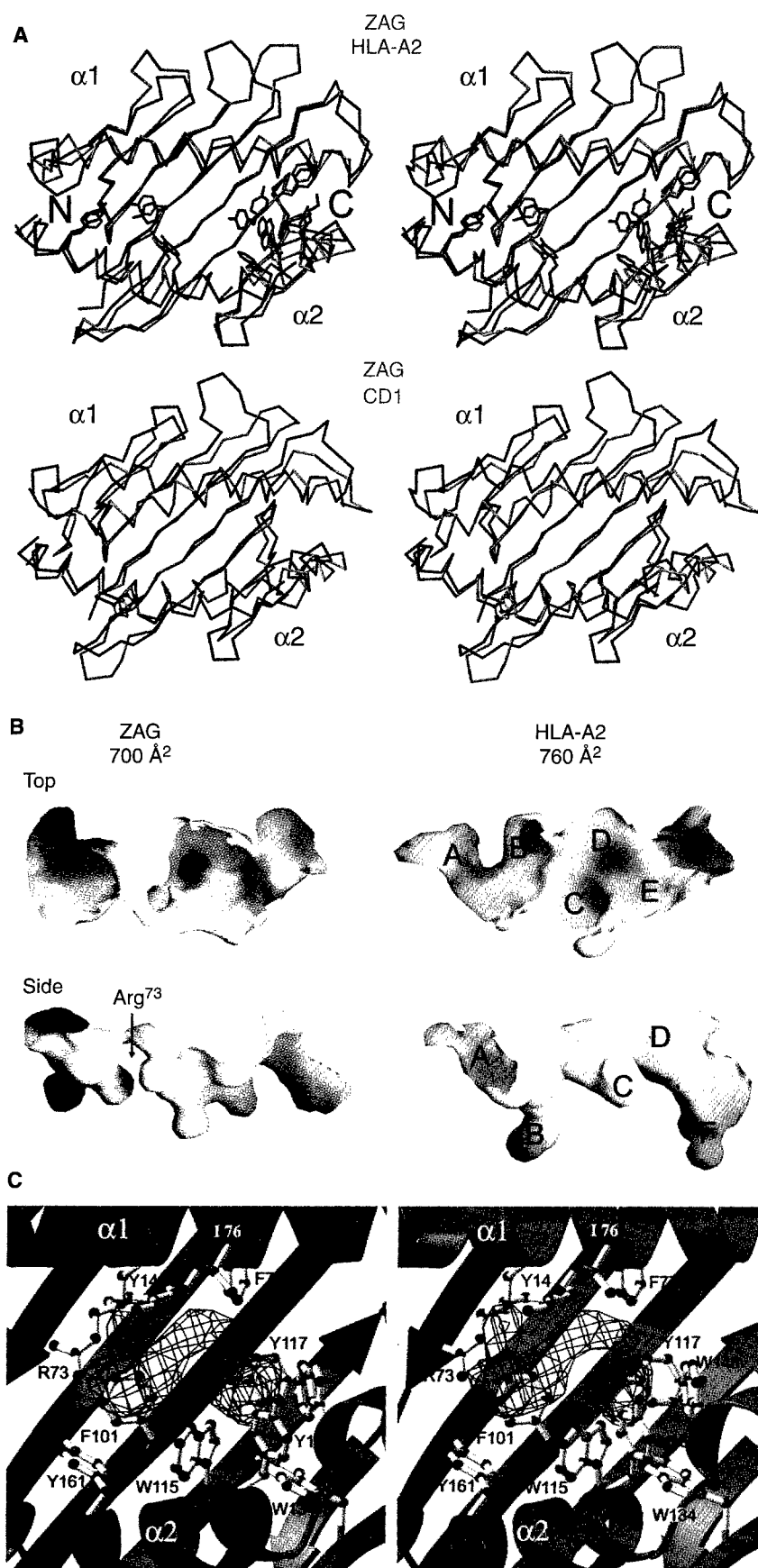
A

ZAG
HLA-A2

ZAG
CD1

B

ZAG
700 Å²

HLA-A2
760 Å²

Top

Side   Arg⁷³

C

Fig. 3. Comparisons of the grooves of ZAG, class I, and class I–related proteins. (**A**) Stereoview comparisons of the $\alpha1$-$\alpha2$ platforms of ZAG and class I proteins that contain open antigen-binding grooves. (Top) ZAG is compared with HLA-A2, a classical class I MHC molecule. "N" and "C" indicate the orientation with respect to the NH_2- and COOH-termini of a peptide bound in the HLA-A2 groove. Side chains in common between the ZAG and HLA-A2 grooves (Table 2) are highlighted on the Cα backbones. Although many of the ZAG groove residues are chemically identical to their counterparts in HLA-A2, the conformations of the side chain, the backbone, or both, of these residues are generally different; thus, the grooves have different shapes [see (B)]. (Bottom) Comparison of ZAG and CD1. Although the ZAG and CD1 grooves both bind nonpeptidic ligands, the ZAG groove is smaller and shallower. Prolines within the $\alpha2$ domain helices of ZAG (Pro¹⁶⁷) and CD1 (Pro¹⁶⁹) are highlighted. The proline in the ZAG helix is accommodated without significant distortion (24), as previously seen for the analogous proline within the HFE helix (Pro¹⁶⁶) (11). (**B**) Extruded groove pockets of ZAG and HLA-A2. Cut-away groove molecular surfaces (11) are shown from above (top) and the side (bottom) with electrostatic potentials (23), in which positive potential is blue, neutral is white, and negative potential is red. The approximate locations of pockets A through F (Table 2) are indicated on the HLA-A2 surfaces. The molecular surface of the central portion of the ZAG groove is nearly neutral except for the contribution of Arg⁷³ and, like CD1 (11), is hydrophobic compared to the grooves of the class I molecules. Calculated groove surface areas (11) are indicated for ZAG and HLA-A2. For comparison, the groove surface areas for other MHC homologs are ~1440 Å² (CD1), ~235 Å² (FcRn), and ~415 Å² (HFE) (11). (**C**) Stereoview of electron density (from a 2.9 Å MIRAS, NCS averaged, figure-of-merit weighted electron density map contoured at 1σ) corresponding to the ZAG ligand superimposed upon a ribbon diagram of the ZAG $\alpha1$-$\alpha2$ platform. Residues within 4.5 Å of the density (Table 2) are highlighted in ball-and-stick representation. Figures were made as described (23).

[FcRn (*11*), HFE (*11*), and MIC-A (*10*)]. Despite the fact that most of the residues within the COOH-terminal portion of the ZAG α2 domain helix are chemically identical to their class I counterparts (Table 2), the ZAG groove has a different shape than a typical class I MHC peptide-binding groove (Fig. 3B). Differences in side chain conformations (Fig. 3A) and side chain substitutions create the altered shape of the ZAG groove, which can be described as containing three pockets: a large, predominantly hydrophobic central pocket and two smaller, more acidic flanking pockets (Fig. 3B). The boundary on the left of the central pocket (Fig. 3B) is created by the side chain of Arg[73], which points into the groove to separate the central and left pockets. Class I MHC grooves contain a smaller side chain at this position (His[70] in

HLA-A2) (*4*). Because of Arg[73] and other side chain substitutions or conformational differences relative to class I molecules, the ZAG groove cannot accommodate even a polyalanine version of an eight- or nine-residue peptide in a class I–binding conformation (Table 2).

Instead of a peptide, the ZAG groove contains an as yet unidentified ligand that cocrystallizes with the protein. Electron density that cannot be accounted for by the amino acid sequence or N-linked carbohydrates is found in the central pocket of the ZAG groove (Figs. 1A and 3C). The density is a curved nonbranched tube, lacking the characteristic protrusions of peptides, that is situated near a cluster of hydrophobic amino acids (three tryptophans, four tyrosines, an isoleucine, and two phenylalanines) and the positively charged side chain of

Arg[73] (Table 2). Although it is not possible to unambiguously identify the compound or compounds in the ZAG groove at the current resolution of the electron density maps, previous biochemical studies rule out that the density corresponds to peptide or mixture of peptides (*9*). The composition of the ZAG groove residues near the density (Table 2) suggests that it represents one or more small hydrophobic molecules, perhaps negatively charged. Chloroform-methanol extractions and acid eluates of ZAG as well as the intact protein have been analyzed by gas chromatography, electrospray, or matrix-assisted laser desorption/ionization mass spectrometry, or a combination of these methods (*22*). The ligand has not yet been detected, but in the absence of information about the chemical nature, size, and ionic state of the ligand, these results cannot be considered conclusive. Electrospray analyses of proteolytic fragments of ZAG reveal that the ligand is not covalently bound (*22*).

Classical class I MHC molecules are extremely polymorphic, whereas ZAG exhibits species-specific variations but little or no genetic polymorphism (*4, 5*). Most of the allele-specific variations of class I MHC molecules map to residues within the peptide-binding groove that interact with peptides (Table 2) (*5*). This property of class I molecules results in allele-specific peptide-binding motifs, such that individual class I molecules show distinct preferences for binding peptides (*5*). In contrast, residues within the ZAG groove are mostly conserved, and those residues closest to the ZAG ligand are completely conserved (Table 2), even though human and rodent ZAG share only ~56% sequence identity (*4*). Taken together with ZAG's lack of polymorphism, these observations imply that human and rodent ZAG carry a single compound, or single class of compounds, related to their function in lipid catabolism.

The crystallographic analysis of ZAG reveals a structure with surprising similarity to classical class I molecules despite ZAG's inability to bind peptides or β2M (*9*). ZAG and MHC-related proteins such as FcRn (*11*) and HFE (*11*) have adapted the same basic fold to perform widely different roles within and outside of the immune system. These molecules illustrate the versatility of the MHC fold and raise intriguing questions about the ancestral function and evolutionary relationships of MHC and MHC-related proteins.

Table 2. Comparison of residues in α1-α2 grooves of ZAG and a class I MHC molecule. Uppercase letters in any of the HLA-A2 and ZAG columns indicate residues that are conserved in human class I MHC sequences (*4*) or residues that are conserved in human, mouse, and rat ZAG (*4*). Pocket residues in the peptide-binding groove of HLA-A2 are defined as having ≥5.0 Å² accessible surface area to a 1.4 Å probe, but <5.0 Å² accessible surface area to a 5 Å probe (*11*). HLA-A2 residues marked with an asterisk were originally defined as pocket residues by M. A. Saper et al. (*11*) but are accessible to a 5.0 Å probe. The HLA-A2 residues designated as "NONE" (conserved) or "none" (not conserved) do not meet the criteria for being in a pocket, but are listed here for comparison with ZAG. Pocket letter names (uppercase letters, conserved residues) refer to well-characterized pockets in the peptide-binding grooves of class I MHC molecules (*5, 11*). ZAG residues analogous to class I pocket residues are designated as "POCKET" (conserved) or "pocket" (not conserved) if they meet the criteria for pocket residues in HLA-A2, "BURIED" or "buried" if they have ≤5.0 Å² accessible surface area to a 1.4 Å probe and ≤5.0 Å² accessible surface area to a 5 Å probe, and "EXPOSED" or "exposed" if they have ≥5.0 Å² accessible surface area to a 1.4 Å probe and ≥5.0 Å² accessible surface area to a 5 Å probe. Surface areas were calculated (*11*) using the coordinates of HLA-A2 (excluding water molecules and bound peptide) and ZAG. Steric clashes with polyalanine peptides bound to ZAG in their class I–binding configuration were defined as described in the structural analysis of HFE (*11*).

HLA-A2	Pocket	ZAG	Pocket	Clash with peptide?	≤4.5 Å of ZAG ligand?
MET-5	A	LEU-10	BURIED	NO	NO
TYR-7	A,B	tyr-12	pocket	yes	no
phe-9	b,c	TYR-14	POCKET	NO	YES
met-45	b	ser-48	pocket	no	no
tyr-59	a	ASP-62	EXPOSED	NO	NO
glu-63	a,b	asp-66	pocket	no	no
lys-66*	a	LEU-69	EXPOSED	YES	NO
val-67	b	GLN-70	POCKET	YES	NO
his-70	b,c	ARG-73	POCKET	YES	YES
thr-73*	c	ILE-76	EXPOSED	YES	YES
his-74	none	PHE-77	POCKET	NO	YES
val-76	none	glu-79	exposed	yes	no
asp-77*	f	THR-80	POCKET	YES	NO
thr-80*	f	ASP-83	EXPOSED	YES	NO
leu-81	f	ILE-84	POCKET	NO	NO
arg-97	c,e	GLY-99	POCKET	NO	NO
tyr-99	a,b,c,d	PHE-101	POCKET	NO	YES
his-114	c,d,e	TRP-115	POCKET	NO	YES
tyr-116	c,f	TYR-117	POCKET	NO	YES
TYR-118	F	TYR-119	POCKET	NO	NO
TYR-123	F	tyr-124	pocket	no	no
ILE-124	F	ILE-125	BURIED	NO	NO
TRP-133	NONE	TRP-134	POCKET	NO	YES
thr-143	f	THR-144	POCKET	YES	NO
LYS-146	NONE	LYS-147	EXPOSED	YES	NO
trp-147	e,f	TRP-148	POCKET	NO	YES
val-152	e	TYR-154	EXPOSED	NO	YES
leu-156	d,e	ALA-158	POCKET	NO	NO
TYR-159	A,D	TYR-161	POCKET	YES	YES
trp-167	a	thr-169	pocket	yes	no
tyr-171	a	TYR-173	POCKET	YES	NO

References and Notes
1. W. Bürgi and K. Schmid, *J. Biol. Chem.* **236**, 1066 (1961); T. Tada et al., *J. Histochem. Cytochem.* **39**, 1221 (1991).
2. N. J. Bundred, W. R. Miller, R. A. Walker, *Histopathology* **11**, 603 (1987); J. P. Freije, A. Fueyo, J. Uría, C. López-Otín, *FEBS Lett.* **290**, 247 (1991); L. M. Sánchez, F. Vizoso, I. Díez-Itza, C. López-Otín, *Cancer Res.* **52**, 95 (1992); I. Díez-Itza et al., *Eur. J. Cancer* **9**, 1256 (1993); Y. S. López-Boado, I. Díez-Itza, J. Tolivia, C. López-Otín, *Breast Cancer Res. Treat.* **29**, 247 (1994).

3. P. T. Todorov et al., Cancer Res. **58**, 2353 (1998); K. Hirai, H. J. Hussey, M. D. Barber, S. A. Price, M. J. Tisdale, ibid., p. 2359.

4. Protein sequences: Human ZAG [T. Araki et al., Proc. Natl. Acad. Sci. U.S.A. **85**, 679 (1988)]; mouse ZAG [H. Ueyama, H. Naitoh, I. Ohkubo, J. Biochem. **116**, 677 (1994)]; rat ZAG [A. Fueyo, J. A. Uría, J. P. Freije, C. López-Otín, Gene **145**, 245 (1994)]. Human class I MHC sequences [P. J. Bjorkman and P. Parham, Annu. Rev. Biochem. **59**, 253 (1990)]; MHC homolog sequences, SWISS-PROT [A. Bairoch and R. Apweiler, Nucleic Acids Res. **26**, 38 (1998)]. Sequence identities: ZAG and HLA-A2, 36%; ZAG and FcRn, 27%; ZAG and mouse CD1d, 23%; ZAG and HFE, 36%; ZAG and MIC-A, 29%.

5. D. R. Madden, Annu. Rev. Immunol. **13**, 587 (1995).

6. E. M. Beckman et al., Nature **372**, 691 (1994); A. R. Castaño et al., Science **269**, 223 (1995).

7. R. P. Junghans, Immunol. Res. **16**, 29 (1997); V. Ghetie and E. S. Ward, Immunol. Today **18**, 592 (1997); N. E. Simister, E. J. Israel, J. C. Ahouse, C. M. Story, Biochem. Soc. Trans. **25**, 481 (1997).

8. J. N. Feder et al., Nature Genet. **13**, 399 (1996); J. N. Feder et al., Proc. Natl. Acad. Sci. U.S.A. **95**, 1472 (1998).

9. L. M. Sánchez, C. López-Otín, P. J. Bjorkman, Proc. Natl. Acad. Sci. U.S.A. **94**, 4626 (1997). In thermal denaturation studies, ZAG denatures with a transition midpoint of 65°C, compared to 57°C for the peptide-filled class I molecule H-2K^d and 45°C for empty K^d [M. L. Fahnestock, I. Tamir, L. Narhi, P. J. Bjorkman, Science **258**, 1658 (1992)].

10. V. Groh et al., Proc. Natl. Acad. Sci. U.S.A. **93**, 12445 (1996). The crystal structure of MIC-A reveals a major rearrangement in domain organization compared to the structures of class I molecules and ZAG. The MIC-A $\alpha1$-$\alpha2$ platform is displaced from its $\alpha3$ domain by 113.5° compared to class I molecules. As a result, the MIC-A $\alpha1$-$\alpha2$ platform makes no contact with its $\alpha3$ domain [P. Li, S. T. Willie, S. Bauer, D. L. Morris, T. Spies, R. K. Strong, personal communication].

11. Protein structures: HLA-A2 [Protein Data Bank (PDB) code 2CLR] [E. J. Collins, D. N. Garboczi, D. C. Wiley, Nature **371**, 626 (1994)]; Mouse CD1 (PDB code 1CD1) [Z.-H. Zeng et al., Science **277**, 339 (1997)]; Rat FcRn (PDB code 3FRU) [W. P. Burmeister, L. N. Gastinel, N. E. Simister, M. L. Blum, P. J. Bjorkman, Nature **372**, 336 (1994)]; Human HFE (PDB code 1A6Z) [J. A. Lebrón et al., Cell **93**, 111 (1998)]. Molecular surface areas buried by interaction were calculated with X-PLOR [A. T. Brünger, X-PLOR. Version 3.1: A System for X-ray and NMR (Yale Univ. Press, New Haven, CT, 1992)] with a 1.4 Å radius. Identification of pocket residues and calculation of groove surface areas were done based upon earlier analyses of human and mouse class I structures [M. A. Saper, P. J. Bjorkman, D. C. Wiley, J. Mol. Biol. **219**, 277 (1991); M. Matsumura, D. H. Fremont, P. A. Peterson, I. A. Wilson, Science **257**, 927 (1992)] as described in the CD1 (Z.-H. Zeng et al.) and HFE (J. A. Lebrón et al.) structure papers. Cut away molecular surfaces of grooves (Fig. 3B) were generated as described in the CD1 structure paper.

12. S. Shibata and K. Miura, Nephron **31**, 170 (1982).

13. Structure determination and refinement: HKL [Z. Otwinowski and W. Minor, Methods Enzymol. **276**, 307 (1997)]. SHARP [E. De La Fortelle and G. Bricogne, ibid., p. 472]. Solomon [J. P. Abrahams and A. G. W. Leslie, Acta Crystallogr. D **52**, 30 (1996)]. CCP4 programs [CCP4: Collaborative Computational Project No. 4, Daresbury, UK, Acta Crystallogr. D **50**, 760 (1994)]. O [T. A. Jones and M. Kjeldgaard, Methods Enzymol. **277**, 173 (1997)]. R_{free} [A. T. Brünger, Nature **355**, 472 (1992)]. The Native II data set (Table 1) was used for refinement. After rigid-body refinement of eight domains in the asymmetric unit ($\alpha1$-$\alpha2$ and $\alpha3$ for each of four ZAG molecules) using CNS [A. T. Brünger et al., Acta Crystallogr. D **54**, 905 (1998)], the four molecules were subjected to restrained NCS torsion-angle refinement using the maximum likelihood target function. Tight NCS restraints (300 kcal/mol·Å²) were applied to all regions except for flexible loops and residues involved in lattice contacts. Intermediate rounds of model building and refinement included the calculation of SIGMAA-weighted [R. J. Read, Acta Crystallogr. A **42**,

140 (1986)] simulated annealing omit maps [A. Hodel, S.-H. Kim, A. T. Brünger, Acta Crystallogr. A **48**, 851 (1992)]. Final rounds of rebuilding and refinement included tightly restrained individual atomic temperature factor refinement (temperature factor rms deviation for bonded main chain and side chain atoms is 5.7 and 8.8 Å², respectively). The model consists of residues 5 through 277 (average B: 48 Å²) with nine carbohydrate residues (average B: 61 Å²) for molecule 1, residues 5 through 278 (average B: 56 Å²) with 11 carbohydrate residues (average B: 80 Å²) for molecule 2, residues 6 through 278 (average B: 57 Å²) with four carbohydrate residues (average B: 107 Å²) for molecule 3, and residues 6 through 249 and 258 through 276 (average B: 62 Å²) with five carbohydrate residues (average B: 90 Å²) for molecule 4 (Wilson B = 64 Å²). Excluding regions that deviate from the NCS, the domains in the NCS-related ZAG monomers are very similar (<0.04 Å rms deviation for Cα atoms). Ramachandran plot statistics (Table 1) are as defined by G. J. Kleywegt and T. A. Jones [Structure **4**, 1395 (1996)].

14. Extensive carbohydrate density is found at Asn^{239} (nine ordered carbohydrate residues in molecule 2) and to a much lesser extent at Asn^{89} and Asn^{108} in all four ZAG molecules (Fig. 1) (13). Crystal structures of glycoproteins rarely show more than three ordered carbohydrate residues at each glycosylation site [D. E. Vaughn and P. J. Bjorkman, Structure **6**, 63 (1998)]. The Asn in the fourth potential N-linked glycosylation site (Asn^{92}) does not show density corresponding to carbohydrate. The bond between Asn^{92} and Gly^{93} can be cleaved by hydroxylamine, confirming that Asn^{92} is not glycosylated (18).

15. M. Takagaki et al., Biochem. Biophys. Res. Commun. **201**, 1339 (1994); O. Ogikubo et al., ibid. **252**, 257 (1998); M. Pfaff, in Integrin-Ligand Interaction, J. A. Eble and K. Kühn, Eds. (Chapman & Hall, New York, 1997), pp. 101–121.

16. V. A. Tysoe-Calnon, J. E. Grundy, S. J. Perkins, Biochem. J. **277**, 359 (1991); D. Lancet, P. Parham, J. L. Strominger, Proc. Natl. Acad. Sci. U.S.A. **76**, 3844 (1979); A. Bauer et al., Eur. J. Immunol. **27**, 1366 (1997).

17. Structural features that prevent ZAG from binding β_2M include the following residues, which clash with

β_2M when it is positioned on the ZAG structure either by interacting with $\alpha3$ or with $\alpha1$-$\alpha2$: Ile^{13}, Thr^{15}, Leu^{30}, Arg^{40}, Gln^{98}, Tyr^{118}, Lys^{122}, Val^{234}, His^{236}, Trp^{245}.

18. L. M. Sánchez and P. J. Bjorkman, unpublished results.

19. G. F. Gao et al., Nature **387**, 630 (1997).

20. D. N. Garboczi et al., ibid. **384**, 134 (1996); K. C. Garcia et al., Science **274**, 209 (1996); Y. H. Ding et al., Immunity **8**, 403 (1998); K. C. Garcia et al., Science **279**, 1166 (1998).

21. Superpositions based on Cα atoms in the platform β strands reveal that the ZAG platform is more similar to classical class I MHC molecules than to any of the class I homologs [rms deviations for superpositions of platforms: ZAG and HLA-A2, 1.3 Å (147 Cα atoms); ZAG and CD1, 1.1 Å (86 Cα atoms); ZAG and FcRn 1.0 Å (88 Cα atoms); ZAG and HFE 1.0 Å (115 Cα atoms)].

22. L. M. Sánchez, A. J. Chirino, P. J. Bjorkman, G. Hathaway, P. G. Green, K. Faull, unpublished results.

23. Figures 1, 2A (right), 2B, 3A, and 3C were made using MOLSCRIPT [P. J. Kraulis, J. Appl. Crystallogr. **24**, 946 (1991)] and RASTER-3D [E. A. Merritt and M. E. P. Murphy, Acta Crystallogr. D. **50**, 869 (1994)]. Electrostatic calculations were done and Figs. 2A (left) and 3B were made using GRASP [A. Nicholls, R. Bharadwaj, B. Honig, Biophys. J. **64**, A166 (1993)].

24. ZAG, CD1, HFE, and FcRn contain prolines within their $\alpha2$ domain helices at a position corresponding to Val^{165} in classical class I MHC molecules (4). The FcRn and CD1 helices are kinked at a position near their proline residues, whereas the ZAG and HFE helices are similar to the $\alpha2$ domain helices of class I molecules (11). Substitution of Val^{165} for proline in the mouse class I molecule H-2D^d did not interfere with binding and presentation of peptides to T cells, suggesting that no major structural rearrangements occurred [D. Plaksin, K. Polakova, M. G. Mage, D. H. Margulies, J. Immunol. **159**, 4408 (1997)].

25. We thank G. Hathaway, P. G. Green, and K. Faull for mass spectrometric analyses. ZAG coordinates have been deposited in the PDB (code 1zag). L.M.S. was supported by a grant from the U.S. Department of Defense Breast Cancer Research Program.